Deformation measurement in the wind tunnel for an UAV leading edge with a morphing mechanism

Radestock, M.; Riemenschneider, J.; Monner, H.P.; Huxdorf, O.; Werter, Noud; De Breuker, Roeland

Publication date
2016

Document Version
Final published version

Published in
30th Congress of International Council of the Aeronautical Sciences

ICAS 2016
30th Congress of the International Council of the Aeronautical Sciences
DCC, Daejeon, Korea ; September 25-30, 2016

DEFORMATION MEASUREMENT IN THE WIND TUNNEL FOR AN UAV LEADING EDGE WITH A MORPHING MECHANISM

Martin Radestock*, Johannes Riemenschneider*, Hans Peter Monner*, Oliver Huxdorf*, Noud P.M. Werter, Roeland De Breuker****
***German Aerospace Center (DLR), ****Delft University of Technology**

Abstract

In a wind tunnel experiment a morphing wing with span extension and camber morphing was investigated. The considered aircraft is an unmanned aerial vehicle (UAV) with a span of 4 m. During the investigations a half wing model was analysed with pressure and structural measurement. The half wing model has three different morphing mechanisms. The focus is on the morphing leading edge concept, which will be shortly described with the main objectives. First of all the morphing leading edge will be described. Afterwards the results of the wind tunnel measurement for pressure distribution, balance and deformation measurement will be presented and discussed.

1 Introduction

Morphing in aircrafts is not a novel idea and there were a lot of investigations for different concepts. An overview is given in [1], [2]. All concepts influence the flight states and have advantages, but also disadvantages. In order to prevent the cons from one concept a combination of different concept can lead to an improved wing configuration. The utility of a concept is a question of the aircraft size and the mission. In the context of the CHANGE project a combination of three different morphing mechanisms in one wing is investigated.

The basic aircraft is an unmanned aerial vehicle (UAV), which is provided by TEKEVER. On the baseline fuselage is a wing mounted, which carries the developed mechanisms. The maximum take-off weight is by 25 kg and the maximum span is 4m.

2 UAV wing concept

The basic concept of the wing is a combination of different morphing mechanisms. These morphing mechanisms are divided into three independent regions, which are represented in Fig. 1 as yellow regions. Each morphing region is a separate module, which is mounted to the wing. Two modules are responsible for camber morphing and the third module realises a span extension of the wing.

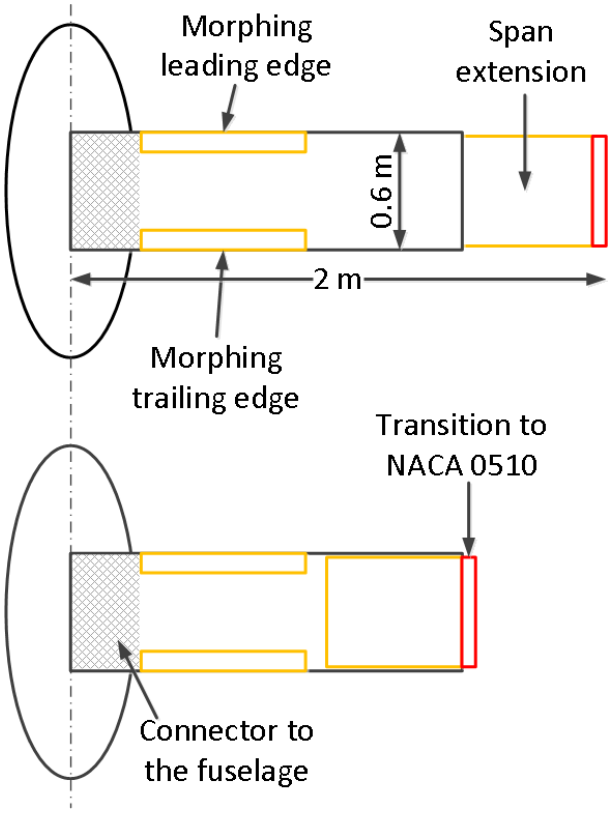

Fig. 1: Modular wing concept in CHANGE

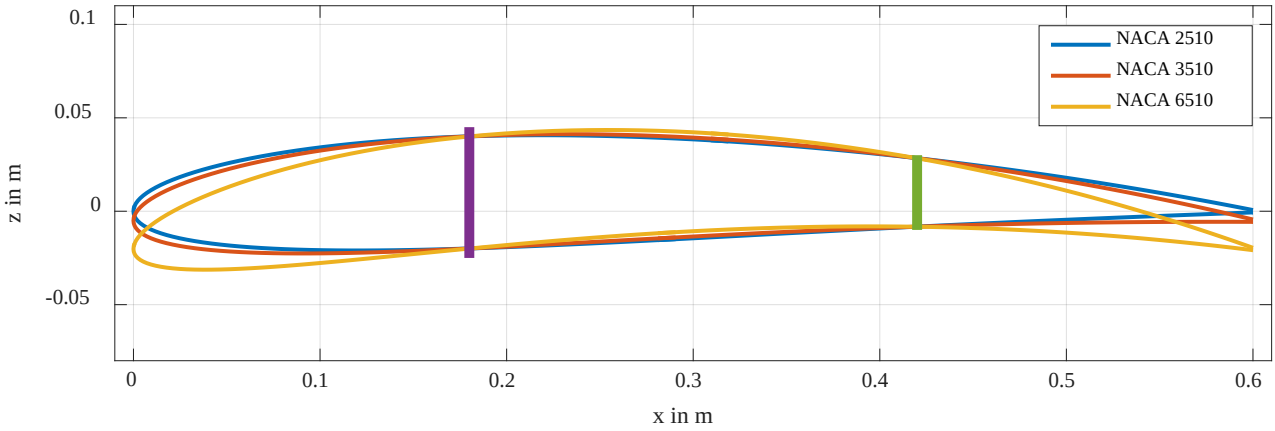

Fig. 2: Aerodynamic shapes out of the optimization [3]

The baseline wing in black is rigid and has cut offs for the morphing leading and trailing edges near to the fuselage. Each cut off has a span of 0.9 m, where the different modules will fit in. The span extension can slide into the hollow wing as illustrated in Fig. 1. The wing planform is rectangular and has a constant profile along the span up to the red transition region. The transition region is a cap, which changes the NACA 6510 profile to the neutral NACA 0510 profile at the wingtip.

2.1 Results of aerodynamic optimization

The design of a morphing mechanism requires aerodynamic shapes, which have to be matched. Out of an aerodynamic optimisation the shapes in Fig. 2 are the resulting NACA shapes [3]. The perpendicular lines in Fig. 2 at chord x = 0.18 m and x = 0.42 m mark the front and rear spar, respectively. The baseline profile is the NACA 6510, because this profile is used for 70% of the flight duration in CHANGE [4]. The region between the spars is assumed to be rigid from NACA 6510 while the leading and trailing edge have to be flexible to enable morphing from NACA 6510 up to NACA 2510 profile. These profiles are the reference for the comparison in the wind tunnel experiment.

2.2 Leading Edge concept

The leading edge concept is an independent module, which is mounted to the cut off of the wing. The top view of the wing in Fig. 3 shows the skin of the leading edge in transparent yellow and its position to the black wing box at the same module position in Fig. 1. There are two independent working red actuation stations in the leading edge marked.

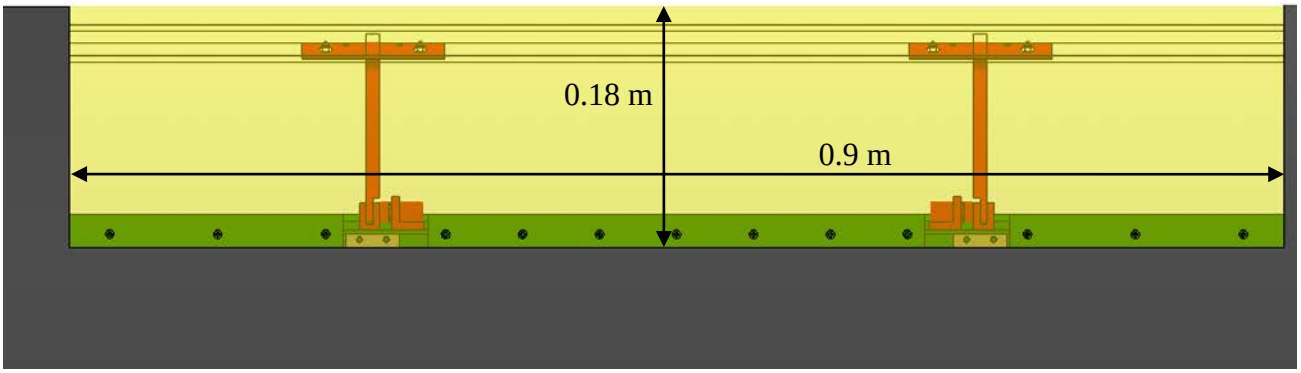

Fig. 3: Top view of the leading edge with two actuation stations in red

These stations reach at different span wise sections different camber variations and produce a twisted profile at the leading edge. This eliminates an additional mechanism in the wing for twist morphing. The morphing module has a span of 0.9 m where the actuation stations are situated 0.225 m from the left and right edge of the module, respectively.

Both actuation stations are equipped with the same mechanism and are represented in Fig. 4. In order to prevent a fine mechanics in the leading edge a compliant mechanism was used. The design process bases on a skin and topology optimization, which is presented in [5]. The first result is a uniform skin made out of three layers glass fibre reinforced plastic (GFRP) and a bottom and top layer out of ethylene propylene diene monomer (EPDM) rubber. The second result is an additive layer manufactured compliant mechanism, which is made out of the thermoplastic material poliactic acid. The kinematic design was post processed manually in the wake of the topology optimization loop [5]. Also the servo motor dimensioning and the interfaces between mechanism, skin, motor and spar are out of a manual design process.

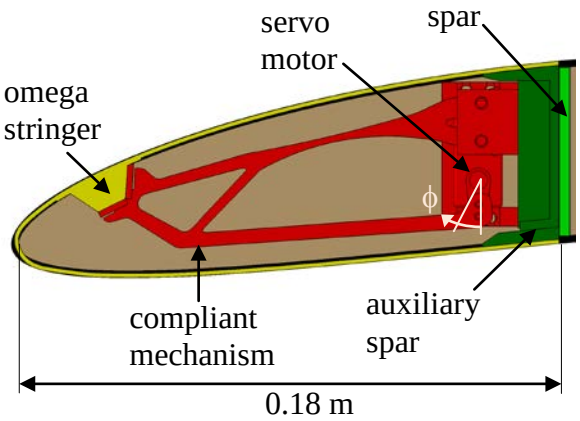

Fig. 4: Side view of the leading edge concept with components

The omega stringer has to be moved in a vertical direction by 12 mm [5]. In this the calculated target shape matches the NACA 2510 profile. The mechanism is similar to a transmission ratio between the servo motor connection and the motion at the omega stringer. So the way at the servo motor reduces to approximately 6 mm in the horizontal direction. The servo motor motion approximates the horizontal movement with an arc. In order to reach the 6 mm the angle at the servo motor is at least $\phi = 30°$.

3 Wind tunnel set up

The prototype wing was tested in the Open Jet Facility (OJF) at the TU Delft at a wind speed of 15 m/s with an extended span and at 28 m/s with a retracted span in order to simulate the low-speed and high-speed configurations. The wind tunnel has an octagonal cross-section of 2.8 m by 2.8 m. Each wing was tested at a range of geometric angles of attack from 0 deg to 10 deg. Note that, since the angles of attack had to be set manually, the results of the shape measurements under no load conditions were used to correct any errors in the geometric angle of attack (AoA) by correlating the position of the wing to the mounting table. Since the wind tunnel is an open jet, the geometric angles of attack have to be corrected further to account for the deflected wind tunnel flow caused by the downwash, resulting in a lower effective angle of attack. Details about these corrections can be found in Glauert [6]. The resulting angles of attack can be found in Table 1 for the baseline configuration and the configuration where the leading edge has been decambered. Note that the actual angle of attack of the morphed wing is slightly different from the actual angle of attack of the baseline wing, since the corrections on the angle of attack are dependent upon the lift coefficient of the wing.

Fig. 5 shows a schematic top view of the wind tunnel setup.

Table 1: Experimental angles of attack

15 m/s	
Baseline	LE morphing
-0.72 deg	-0.72 deg
3.88 deg	3.87 deg
6.63 deg	6.63 deg
8.68 deg	8.69 deg

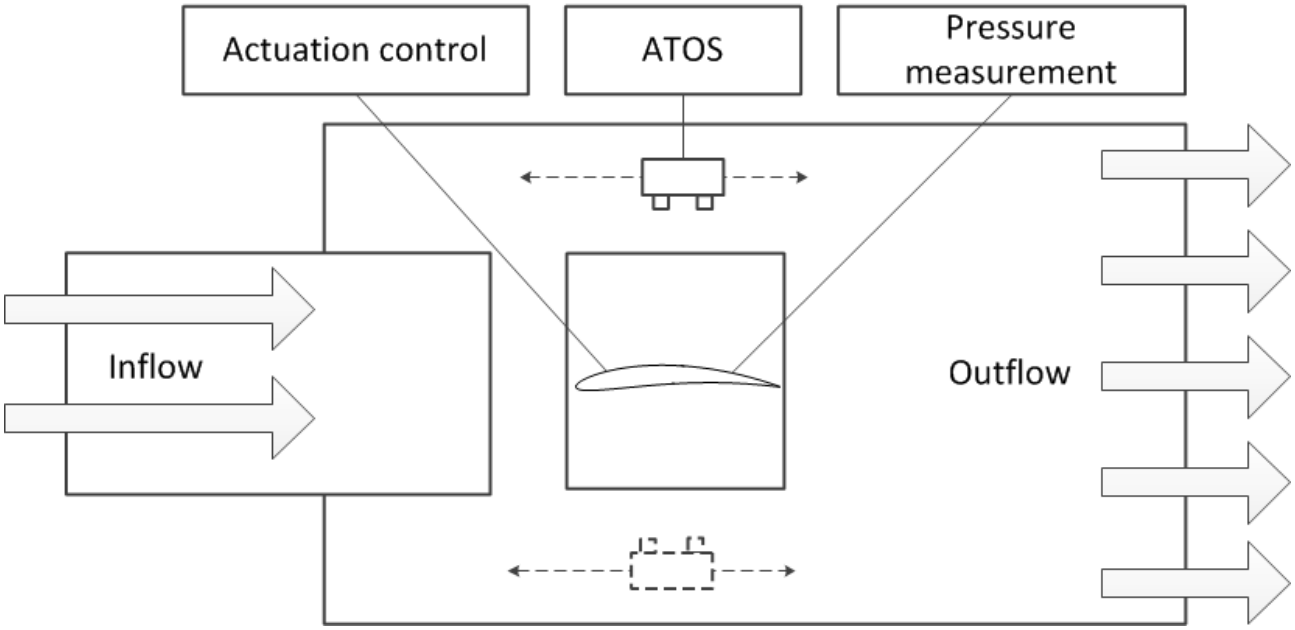

Fig. 5: Schematic overview of the wind tunnel setup

3.1 Aerodynamic measurement

For each measurement point, aerodynamic forces and moments are measured at the root using a 6-component balance and pressures were measured using a Measurement Specialties DTC Initium system with an accuracy of ±0.05% and several Measurement Specialties ESP-HD pressure scanners with an accuracy of ±0.03%. The chordwise and spanwise pressure tap locations on the leading edge are given in Fig. 6 and Fig. 7, respectively.

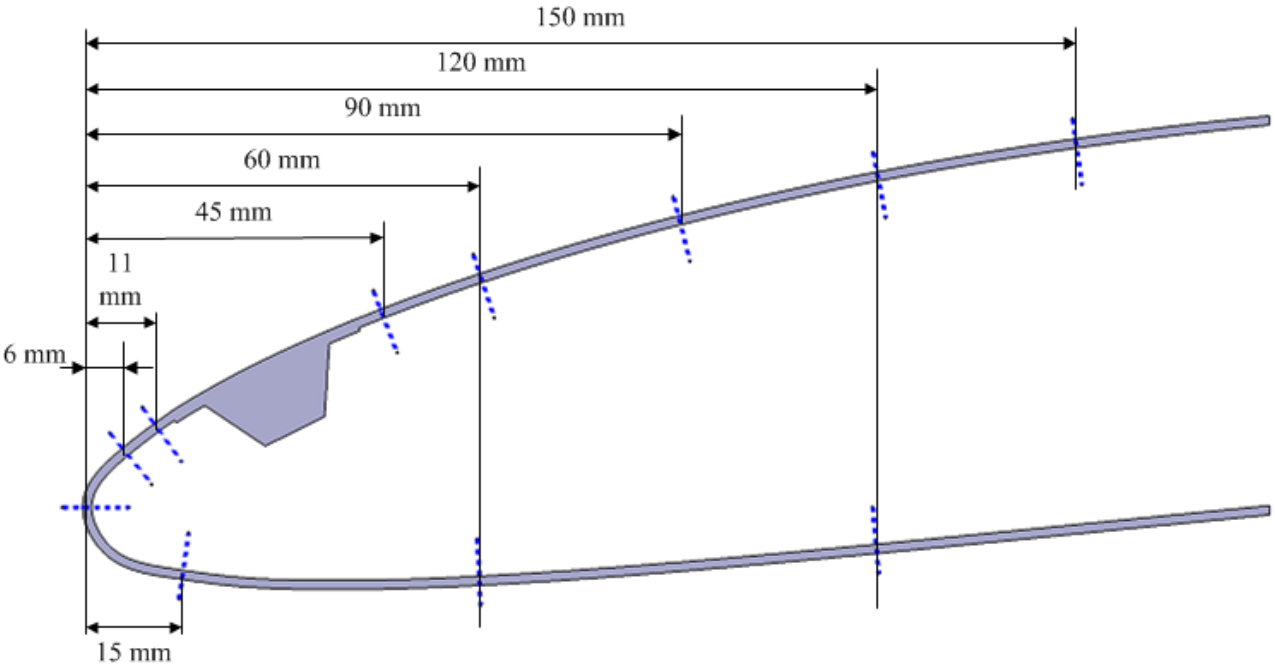

Fig. 6: Chordwise pressure tab locations on the leading edge

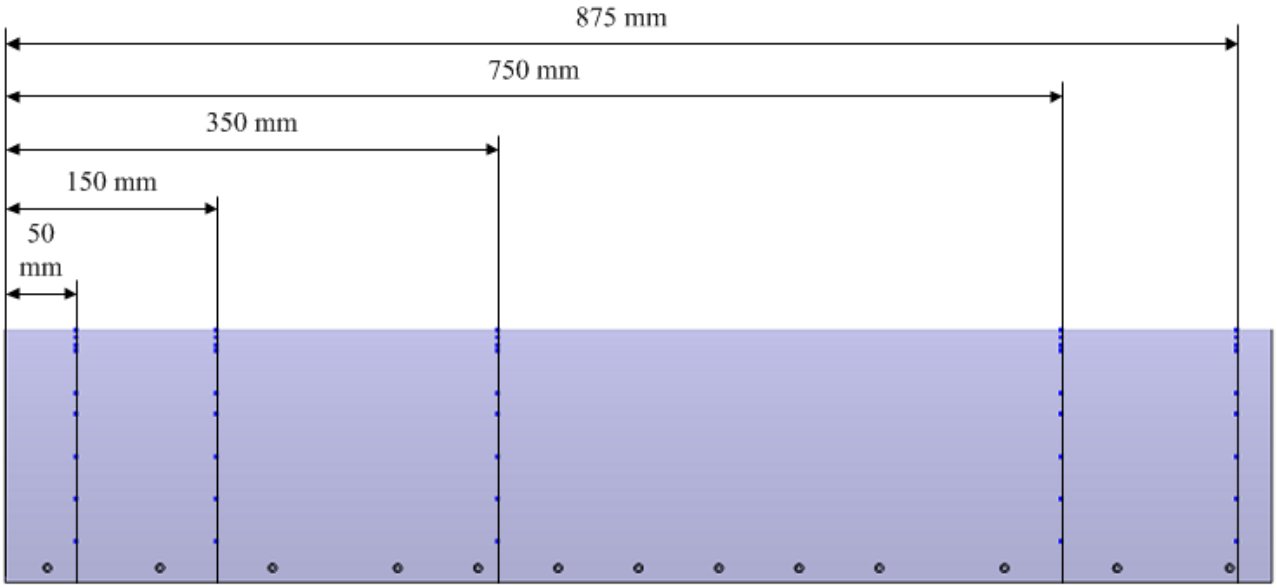

Fig. 7: Spanwise pressure tab locations on the leading edge

3.2 Structural measurement

The possibility for structural measurement without any influence to the flow or to the stiffness of the structure is limited. For this wind tunnel measurement an optical photogrammetric measurement system using a fringe projection was used to digitalise the surface of the half wing model during the aerodynamic measurement. The system is called ATOS provided by GOM Ltd. The sensor with the two cameras is indicated in the schematic overview of the wind tunnel in Fig. 5. In order to scan the whole profile the sensor head has to be moved to both sides of the profile. The scans from suction and pressure side are set together using another system called TRITOP. Therefore calibrated bars and crosses are laid on the table as well as reference marks are stuck on the half wing model.

The system was used to measure the angle of attack, because the adjustment of the model was done manually with a plate where the angles are marked. The half wing model was clamped in this plate and hangs approximately 50 mm above a fixed table. Two reference marks are directly stuck on the table under the foremost and the rearmost point of the wing model in chord direction. The global coordinate system of the surface measurement is oriented with reference marks on the pressure side of the wing. Now the two marks on the table changes their position relative to the global coordinate system and the line between these two points form an angle to the chord of the profile and the angle of attack can be calculated out of the structural measurement. It should be noticed, that the angle out of the ATOS is used as a relative variable for different angles of attack.

4 Measurement results

The section will include separate analysation for aerodynamic and structural measurement in order to show the specifically results for lift coefficient, pressure distribution of the wing model and the profile contour of the leading edge.

4.1 Aerodynamic results

In order to investigate the effect of the leading edge morphing concept on the aerodynamic response of the prototype wing, first, the balance measurements of the morphed

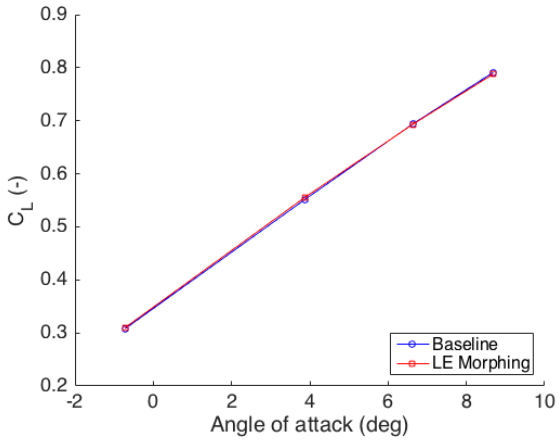

Fig. 8: Balance measurements with and without leading edge morphing

configuration will be compared to the balance measurements of the baseline configuration. The main purpose of leading edge morphing is to postpone stall by affecting the suction peak at the leading edge by changing the local camber and hence angle of attack at the leading edge, and not necessarily to change the aerodynamic loads on the wing. This can also be concluded from Fig. 8 showing a comparison between the balance measurements for the prototype wing in the baseline configuration and the configuration where the leading has been decambered. As can be seen, the effect of leading edge morphing on the overall aerodynamic load on the wing is negligible.

However, the effects of leading edge morphing can clearly be observed, when looking at the pressure measurements in Fig. 9 showing the pressure distributions at different angles of attack. As can be expected, at positive angles of attack, the leading edge suction peak is increased by decambering the leading edge, since the local angle of attack at the leading edge is increased, while at negative angles of attack, the opposite happens, since decambering actual decreases the local angle of attack. Therefore the aerodynamic moment will be

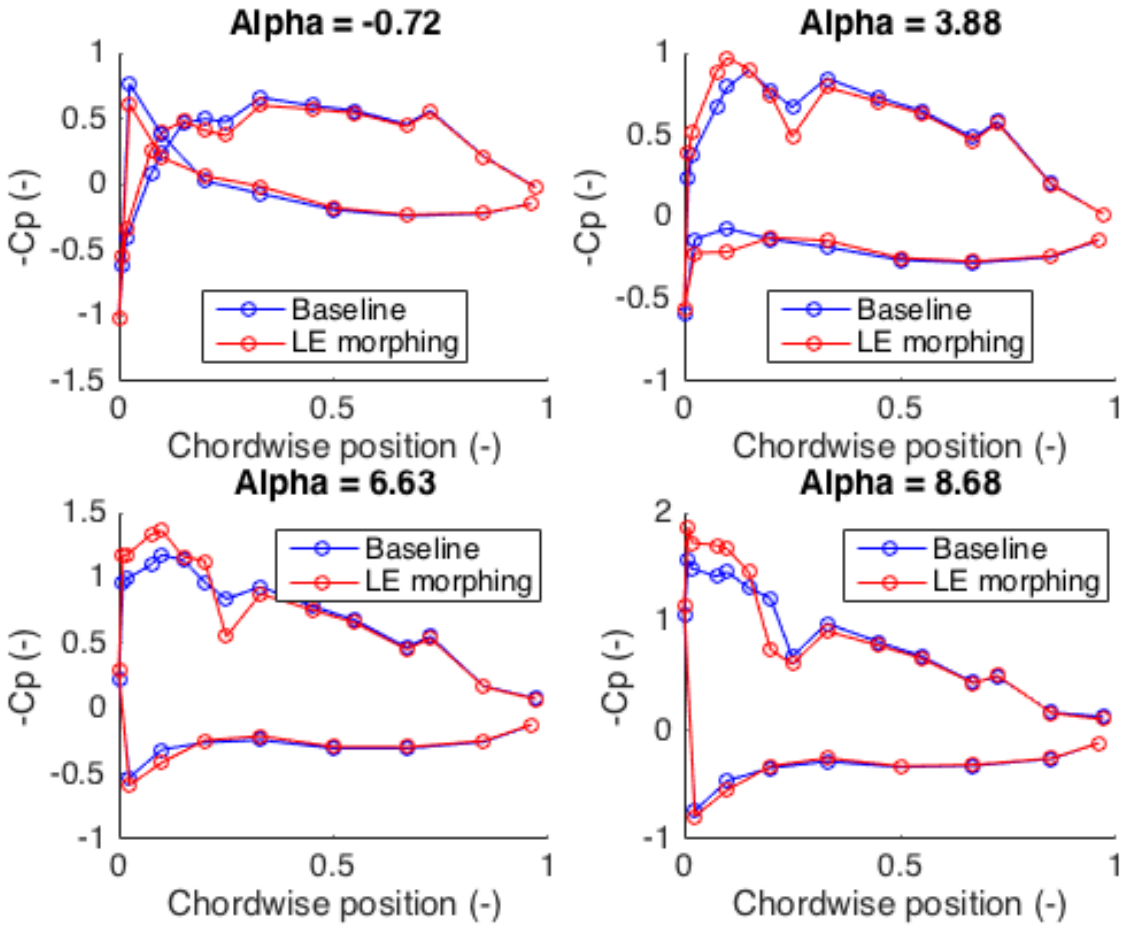

Fig. 9: Pressure measurements at the center of the morphing section at different angles of attack.

affected in contrast to the total aerodynamic load.

It can be observed that an increase in leading edge suction peak is accompanied by a decrease in pressure over the remainder of the airfoil. As a result, as was already observed in the balance measurements, the corresponding lift generated is almost unaffected, as can also be concluded from Table 2: Experimental lift coefficients and leading edge moment coefficient obtained from the pressure distributions. showing the corresponding local lift coefficients obtained by integrating the pressure distributions. Leading edge morphing, however, does affect the local twisting moment.

Table 2: Experimental lift coefficients and leading edge moment coefficient obtained from the pressure distributions.

	Baseline		LE Morphing	
AoA	C_l	$C_{m,LE}$	C_l	$C_{m,LE}$
-0.72 deg	0.44	-0.26	0.44	-0.25
3.88 deg	0.75	-0.33	0.75	-0.31
6.63 deg	0.93	-0.36	0.93	-0.34
8.68 deg	1.03	-0.37	1.02	-0.36

4.2 Structural results

The presented results will only show the structural behaviour at the leading edge with the angle of attack -0.72 deg. At first the whole model with all data points is represented in Fig. 10 and their connection as a surface.

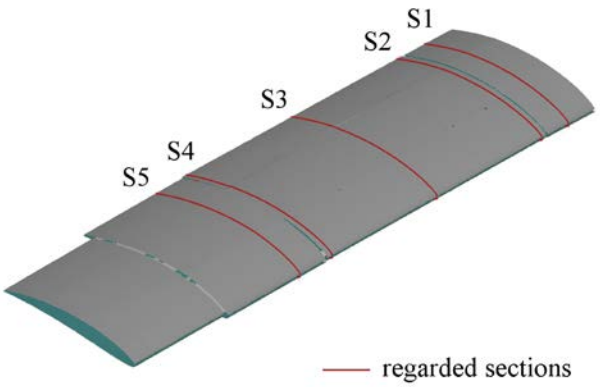

Fig. 10: Analyzed sections from the wing with the ATOS system

In order to show some results from the structural measurement the profile is divided into five sections from S1 to S5. Thereby the sections S1 and S5 are at the fixed wing position where the skin does not have any morphing mechanisms. The sections S2, S3 and S4 show the morphing mechanisms in the baseline and maximum deflected position, which are equal to NACA 6510 and NACA 2510 profile, respectively. The section S2 is near to the edge of the morphing part at the wing root, section S3 is in the middle of the morphing module and section S4 is at the edge of the morphing part near to the wing tip. Regarding the aerodynamic results the section S3 represents the analysed section of the wing for pressure distribution.

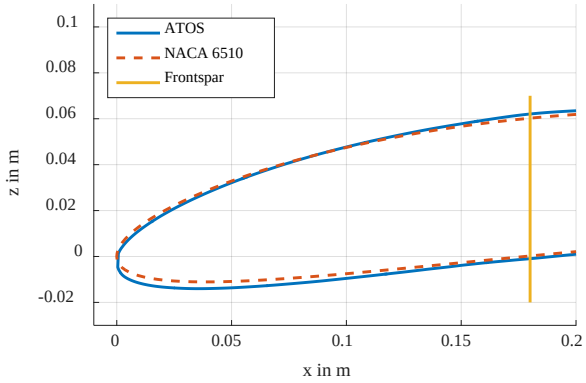

Fig. 11: Comparison between measured and theoretical shape for fixed section S1

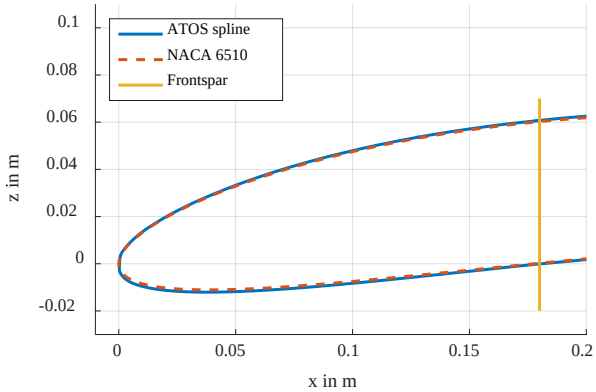

Fig. 12: Comparison between measured and theoretical shape for fixed section S5

In Fig. 11 and Fig. 12 the sections S1 and S5 compared to the baseline profile NACA 6510 is shown, respectively. It can be seen that at section S1 is a divergence of approximately 2.5 mm to the theoretical profile and at section

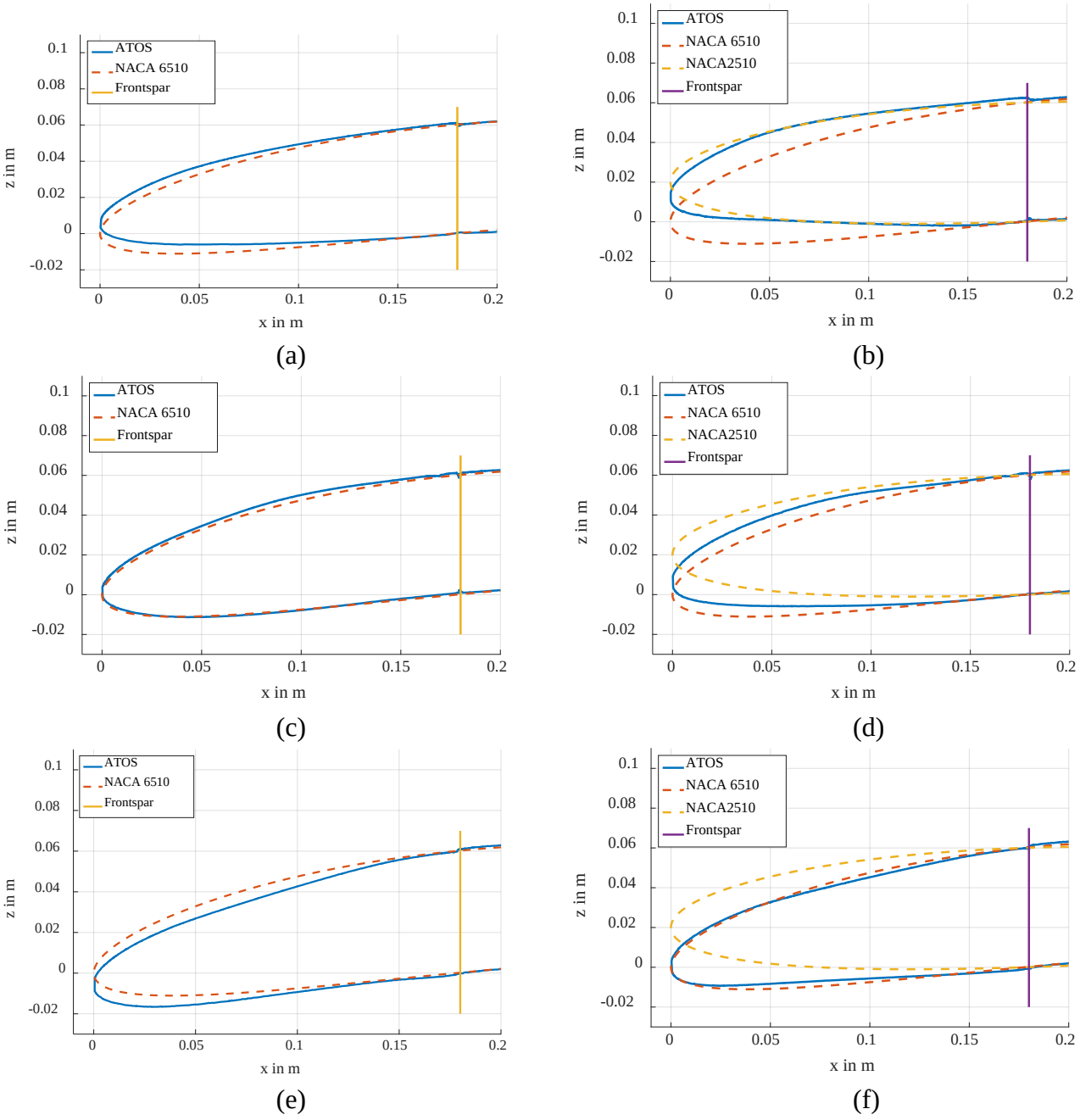

Fig. 13: Surface measurement for (a) baseline section S2, (b) morphed section S2, (c) baseline section S3, (d) morphed section S3, (e) baseline section S4, (f) morphed section S4

S5 it is nearly 1 mm. Both maxima are on the lower side of the profile. This already indicates the manufacturing tolerances for the half wing model at the fixed part.

The difference increases between the manufactured wing model and the theoretical shape, when the morphing module is considered. Fig. 13 (a), (c), (e) shows the morphing module along the span and a twist in the module can be observed in the initial position. The mismatch of the shapes is in Fig. 13 (e) approximately 11 mm near to the front of the leading edge.

This results in a decreased performance for the morphing. The Fig. 13 (b), (d), (f) shows the morphed leading edge with the comparison of the NACA 2510 as target and NACA 6510 as baseline profile. It can be observed that none section match the target profile with a less divergence of 1mm. The actuation seems to be

too weak for the morphing, because all morphed sections are below the NACA 2510 profile. Also the initial twist along the span minimizes the morphing of the mechanism and this results e.g. Fig. 13 (e) to Fig. 13 (f) that the morphing compensate the manufacturing failure of the skin. So the minimal deflection of the leading edge leads to the negligible effect in the balance measurement, which was shown in Fig. 8. Only the pressure distribution for section S3 in Fig. 9 shows the influence of morphing for this leading edge.

5 Conclusions

The results of the wind tunnel measurement show that a morphing leading edge for an UAV has an influence to pressure distribution on the profile. The model itself does not have a major influence on the balance measurement due to small deformation requirements at the leading edge and the low wind speed of 15 m/s. Also the tested morphing module does not deliver satisfying results in the deformation measurement. Due to manufacturing tolerances the wing model has a high difference in the initial shape compared to the theoretical shape, if the dimension of the wing is considered.

The wind tunnel experiment shows the general capability of the morphing mechanism for an UAV leading edge. In order to improve the concept, mostly the manufacturing tolerances and more powerful actuation are necessary to reach the target shapes. Due to the one and only wind tunnel experiment, a modification of the morphing concept cannot be investigated once again in the context of the CHANGE project.

References

[1] Vasista, S., Tong, L., Wong, K. C. Realization of morphing wings: a multidisciplinary challenge. *Journal of Aircraft*, Vol. 49, No. 1, S. 11-28, 2012.

[2] Barbarino, S., et al. A review of morphing aircraft. *Journal of Intelligent Material Systems and Structures*, Vol. 22, No. 9, S. 823-877, 2011.

[3] Ciarella, A., et al. A Multi-Fidelity, Multi-Disciplinary Analysis and Optimization Framework for the Design of Morphing UAV Wings. *AIAA Aviation 2015: Multidisciplinary Analysis and Optimization Conference*. Dallas, Texas, USA, June 2015.

[4] Ciarella, A., Hahn, M., Wong, P., Peace, A., Comparison of Aerodynamic Design Methodologies for Morphing UAV Wings, *Proceedings of the 7th Ankara International Aerospace Conference*. Ankara, Turkey, September 2013.

[5] Radestock, M., et al. Experimental Investigation of a Compliant Mechanism for an UAV Leading Edge. *SMART 2015. 7th Eccomas thematic conference on Smart Structures and Materials.* Ponta Delgada, Acores, Portugal, June 2015.

[6] Glauert H. Wind Tunnel Interference on Wings, Bodies and Airscrews. *Aeronautical Research Committee*, ARC-1566, 1933.

Copyright Statement